

# Ion-Exchange Reactions and Photothermal Patterning of Monolayer Assembled Polyacrylate-Layered Double Hydroxide Nanocomposites on Solid Substrates

Jong Hyeon Lee,<sup>†</sup> Seog Woo Rhee,<sup>‡</sup> and Duk-Young Jung<sup>\*,†</sup>

Department of Chemistry-BK21, Institute of Basic Sciences, Sungkyunkwan Advanced Institute of Nanotechnology, Sungkyunkwan University, Suwon 440-746, Korea, and Department of Chemistry, College of Natural Sciences, Kongju National University, Kongju 314-701, Korea

Received February 3, 2006. Revised Manuscript Received July 25, 2006

Hydrotalcite-like, layered double hydroxide  $[\text{Mg}_4\text{Al}_2(\text{OH})_{12}]\text{CO}_3 \cdot n\text{H}_2\text{O}$  (LDH) nanocrystals immobilized on solid substrates were incorporated with anionic polymers as host matrixes in the intercalation of polyacrylates to produce polymer–inorganic hybrid nanocomposites films on the substrates. The novel functional hybrid films were prepared through a direct ion-exchange reaction of poly(acrylic acid) (PAA) macromolecules into the immobilized LDH in binary solvent systems at 120 °C. SEM images reveal that designed solvent mixing such as alcohol and toluene prevents dissolution of LDH compounds, preserving the high crystallinity of PAA-LDH materials after anion-exchange reaction. X-ray diffraction spectra for polymer/LDH nanohybrids materials gave interlayer spacing of 22 Å regardless to the starting materials with different molecular weights, suggesting a molecular modeling of polymer species in gallery space of LDH. The UV-light decomposition of PAA-LDH composite nanocrystals on Si changes their thickness, restoring their pristine basal spacings. This study describes tailoring of PAA-LDH composite systems on the solid substrates and their applications in light-induced patterning.

## Introduction

There is considerable interest for the development of polymer–inorganic nanocomposites to improve physical and chemical characteristics of multifunctional materials. These nanocomposites can be considered as being reinforcement of polymers or as the synergetic new materials in inorganic frames. Many LDH compounds as host materials present a large variety of compositions and tunable layer charge density.<sup>1</sup> Especially, applications of polymer–LDH nanocomposites expect enhanced mechanical properties, flame retardant properties, bio-LDH nanohybrids, polymer electrolytes, and biological/environmental applications.<sup>2–4</sup> The achievement of such synergetic physicochemical properties is very reliable on the platform of polymer–inorganic hybrid films organized on solid substrates. Hybrid films also are strongly considered to be useful candidates of great capability for developing optical devices, catalysts, and chemical and biosensors.<sup>5–7</sup>

Several polymer incorporation methods have been developed for preparing polymer–LDH nanocomposites, such as synthesis of LDH in polymer solutions, restacking of exfoliated LDH in polymer solution, in situ polymerization of intercalated monomer in LDH, or by direct intercalation of high-molecular-weight macromolecules by ion-exchange reaction.<sup>8–12</sup> The polymer–LDH materials based on restacking and reconstruction of hydroxide layers over the polymers as a self-assembly process generally gave rise to ill-defined LDH–polymer nanocomposites, even when the polymer of polar functional groups such as those including poly(acrylic acid), poly(vinylsulfonate), and poly(stylenesulfonate) were used,<sup>11a</sup> because the polymer insertion affects not only the crystallinity but also the dimension and morphology of the pristine LDH host material. The low crystallinity and

\* Corresponding author. E-mail: dyjung@skku.edu. Fax: +82-31-290-7075.  
<sup>†</sup> Sungkyunkwan University.

<sup>‡</sup> Kongju National University.

- (1) (a) Kahn, A. I.; O'Hare, D. *J. Mater. Chem.* **2002**, *12*, 3191 and references therein. (b) Newman, S.; Jones, W. *New J. Chem.* **1998**, 105. (c) De Ray, A.; Forano, C.; El Malki, K.; Besse, J.-P. In *Synthesis of Microporous Materials*; Occelli, L.; Robson, H., Eds.; Van Nostrand Reinhold: New York, 1992; Vol. 2, p 108.
- (2) Ogawa, M.; Kuroda, K. *Chem. Rev.* **1995**, *95*, 399.
- (3) Ding, W.; Gu, G.; Zhong, W.; Zang, W. C.; Du, Y. *Chem. Phys. Lett.* **1996**, *262*, 259.
- (4) Choy, J. H.; Kwak, S. Y.; Jung, Y. J.; Park, J. S. *Angew. Chem., Int. Ed.* **2000**, *39*, 4042.
- (5) Loy, D. A. *MRS Bull.* **2001**, *26*, 364.
- (6) Darder, M.; López-Blanco, M.; Aranda, P.; Leroux, F.; Ruiz-Hitzky, E. *Chem. Mater.* **2005**, *17*, 1969.

- (7) O'Hare, D. *New J. Chem.* **1994**, *18*, 989.
- (8) (a) Leroux, F.; Besse, J.-P. *Chem. Mater.* **2001**, *13*, 3507. (b) Alexanre, M.; Dubois, P. *Mater. Sci. Eng.* **2000**, *28*, 1.
- (9) (a) Vaysse, C.; Guerlou-Demourgues, L.; Duguet, E.; Delmas, C. *Inorg. Chem.* **2003**, *42*, 4559. (b) Roland-Swanson, C.; Besse, J.-P.; Leroux, F. *Chem. Mater.* **2004**, *16*, 5512. (c) Leroux, F.; Meddar, L.; Mailhot, B.; Morlat-Therias, S.; Gardette, J. *Polymer* **2005**, *46*, 3571.
- (10) (a) Hsueh, H. B.; Chen, C. Y. *Polymer* **2003**, *44*, 1151. (b) Hsueh, H. B.; Chen, C. Y. *Polymer* **2003**, *44*, 5275. (c) Whilton, N. T.; Vickers, P. J.; Mann, S. J. *Mater. Chem.* **1997**, *7*, 1623. (d) Rey, S.; Mérida-Robles, J.; Han, K. S.; Guerlou-Demourgues, L.; Delmas, C.; Duguet, E. *Polym. Int.* **1999**, *48*, 277.
- (11) (a) Oriakhi, C. O.; Faar, I. V.; Lerner, M. M. *J. Mater. Chem.* **1996**, *6*, 103. (b) Laycock, D. E.; Collacott, R. J.; Skelton, D. A.; Tchir, M. F. *J. Catal.* **1991**, *130*, 354. (c) Itoh, T.; Shichi, T.; Yui, T.; Takahashi, H.; Takagi, K. *Chem. Lett.* **2004**, *33*, 1268. (d) Messersmith, P. B.; Stupp, S. I. *Chem. Mater.* **1995**, *7*, 454.
- (12) (a) Wang, G. A.; Wnag, C. C.; Chen, C. Y. *J. Inorg. Organomet. Polym. Mater.* **2005**, *15*, 239. (b) Chen, W.; Feng, L.; Qu, B. *Solid State Commun.* **2004**, *130*, 259. (c) Li, B.; Hu, Y.; Liu, J.; Chen, Z.; Fan, W. *Colloid Polym. Sci.* **2003**, *281*, 998.

unnecessary interparticle polymer of LDH–polymer composites were inevitable in the previous preparation methods, which hampered their detailed microstructural analyses.

In addition, the most common preparation method is based on the anionic exchange of LDH as well as precipitation reaction from nitrate- and chloride-salt precursors in the presence of dissolved anionic species, because the carbonate form of LDH has a very strong affinity to the hydroxide layers, resulting in low reactivity to additional anionic-exchange reaction. These critical reaction conditions exclude carbon dioxide from the atmosphere, causing many inconvenience and limiting a versatile variation of the exchange reaction.

Most anionic-exchange reactions have been achieved in aqueous solutions because of the utilization of water-soluble ionic compounds.<sup>13</sup> The dissolution–recrystallization from the hydrolysis of LDH host layers could be suppressed by using nonaqueous solvents.<sup>14</sup> Recently, we developed an anisotropic 2D monolayer assembly of the LDH nanocrystals on solid surfaces without chemical linkers and demonstrated that the solvothermal anion exchange of dicarboxylate in nonaqueous solvents was able to prevent the dissolution resulting from hydrolysis of the host layers of LDH, where the morphology of LDH particles could be preserved during the reactions.<sup>15</sup> The solvothermal reaction of LDH nanocrystals in organic solvents offers not only solubility of polyacrylic acids but also a large open space for high diffusion rates into the LDH interlayer space, an especially crucial problem in macromolecules. The direct exchange of anionic polymers in the LDH gallery space is also considered to be difficult to achieve because of the low diffusion of polymers and high charge density of the layers.<sup>8a</sup>

In the present study, we report a novel route for preparing polymer–LDH hybrid films with a good crystallinity and a high density of polymer guest by a direct exchange of polymeric macromolecules with carbonate ions through solvothermal reaction. We investigated the immobilized polymer–LDH nanocomposites on substrates under various solvothermal reaction conditions such as reaction media, reaction time, and temperature, which gives useful functional coatings for chemical sensors and electrodes.<sup>16</sup> The anion-exchange reactions using immobilized LDH nanocrystals provide several advantages. First, we could use a very small amount of LDH samples to study anion-exchange reactions. Second, we could easily observe anisotropic variation of the interlayer spacings of LDH by using XRD and SEM techniques. Third, the LDH/Si systems allow us to have a polymer-free surface and to observe morphological changes

of polymer–LDH nanocomposites in the reactions, which is usually difficult in powder samples.

## Experimental Section

PAA with molecular weights 2 and 1250 kD from Aldrich were used as received. The carbonate form of LDH,  $[\text{Mg}_4\text{Al}_2(\text{OH})_{12}]\text{CO}_3 \cdot n\text{H}_2\text{O}$ , denoted as MgAl-LDH, was prepared by the coprecipitation method.<sup>17</sup> To an aqueous solution containing 0.02 M  $\text{Mg}(\text{NO}_3)_2$  and 0.01 M  $\text{Al}(\text{NO}_3)_3$  was slowly added a mixed solution of 2.0 M NaOH and 0.2 M  $\text{Na}_2\text{CO}_3$  with vigorous stirring. During the titration, the pH of the solution was adjusted to  $10.0 \pm 0.1$  at room temperature. The resulting precipitate was collected by centrifugation and washed with deionized water three times. Hydrothermal treatment was carried out in deionized water at 180 °C to obtain a larger crystal size and improved crystallinity of MgAl-LDH crystals, followed by drying at 120 °C in a convection oven.<sup>18</sup>

Immobilization of MgAl-LDH nanocrystals was performed on clean silicon (100) wafers and gold-coated silicon (100) wafers as a substrate. The MgAl-LDH crystals (10 mg) were suspended in dry organic solvents (20 mL) such as 1-butanol or 2-propanol in the covered laboratory glass flask; the flask was then immersed in an ultrasonic bath (95 W, 28 kHz) under ambient pressure at room temperature. The Si and gold-coated silicon substrates cleaned with oxygen plasma (Harrick, 30 W) were dipped in the colloidal suspension of MgAl-LDH and coated with LDH by ultrasonic treatment for 2 min. The LDH coated samples were treated with sonication for an additional minute in 1-butanol or 2-propanol to lift off the excess LDH crystals from the substrates and were dried at 70 °C in air.

The samples coated by MgAl-LDH crystals were transferred into a Teflon-coated autoclave vessel containing a solution of 10 mg of PAA in a binary mixture of ethanol and toluene, e.g., 0.5% (v/v), and heated at 120 °C for 6–48 h. The residual acids on the substrates were washed with ethanol, and the samples were dried at 70 °C in air; the samples were denoted as PAA(L)-LDH and PAA(H)-LDH, according to the low- (2 kD) and high- (1250 kD, 0.1% cross-linked polymer) molecular-weight PAA samples used as starting materials. A thermolysis reaction of polymer–LDH by UV-light radiation was performed on PAA(L)-LDH film using a high-pressure Hg lamp (600 W) under ambient conditions at room temperature for 1 h. Micropatterned structures of PAA(L)-LDH films were prepared by UV irradiation using an Al metal shadow mask and a chromium metal-patterned quartz photo mask.

X-ray diffraction (XRD) patterns were measured with a Rigaku X-ray diffractometer, D/MAX-2000 Ultima, on a  $\theta$ – $2\theta$  scanning mode. The measurements were performed under the conditions of 40 kV, 30 mA, and Cu K $\alpha$  ( $\lambda = 1.5405 \text{ \AA}$ ). All XRD spectra were calibrated using Si (200) peak from substrates ( $2\theta = 32.9^\circ$ ,  $d = 2.74 \text{ \AA}$ ). SEM images were obtained on a Philips XL30. The FT-IR spectra were obtained with a vacuum optics available spectrometer, IFS 66 v/s, Bruker, with a resolution of  $4 \text{ cm}^{-1}$  and a photovoltaic liquid-cooled MCT detector.

## Results and Discussion

**LDH Deposition on the Substrates.** The diameter of the prepared MgAl-LDH disk type powder samples ranges from 100 to 500 nm and the thickness is about 100 nm. In order

- (13) (a) Meyn, M.; Beneke, K.; Lagaly, G. *Inorg. Chem.* **1990**, *29*, 5201. (b) Fogg, A. M.; Dunn, J. S.; Shyn, S. G.; Cary, D. R.; O'Hare, D. *Chem. Mater.* **1998**, *10*, 351. (c) Fogg, A. M.; Dunn, J. S.; O'Hare, D. *Chem. Mater.* **1998**, *10*, 356. (d) Fogg, A. M.; Freij, A. J.; Parkinson, G. M. *Chem. Mater.* **2002**, *14*, 232.
- (14) (a) Boclair, J. W.; Braterman, P. S. *Chem. Mater.* **1999**, *11*, 298. (b) Hibino, T.; Tsunashima, A. *Chem. Mater.* **1997**, *9*, 2082.
- (15) (a) Lee, J. H.; Rhee, S. W.; Jung, D. Y. *Chem. Comm.* **2003**, 2740. (b) Lee, J. H.; Rhee, S. W.; Jung, D. Y. *Chem. Mater.* **2004**, *16*, 4774.
- (16) (a) Thompson, M. E. *Chem. Mater.* **1994**, *6*, 1168. (b) Mallouk, T. E.; Gavin, J. A. *Acc. Chem. Res.* **1998**, *31*, 209. (c) Itaya, K.; Chang, H. C.; Uchida, I. *Inorg. Chem.* **1987**, *26*, 624. (d) Mousty, C.; Therias, S.; Forano, C.; Besse, J.-P. *J. Electroanal. Chem.* **1994**, *374*, 63. (e) Shan, D.; Cosnier, S.; Mousty, C. *Anal. Chem.* **2003**, *75*, 3872.

- (17) (a) Miyata, S. *Clays Clay Miner.* **1983**, *31*, 305. (b) Miyata, S.; Okada, A. *Clays Clay Miner.* **1977**, *25*, 14.
- (18) Hickey, L.; Klopogge, J. L.; Frost, R. L. *J. Mater. Sci.* **2003**, *35*, 4347.

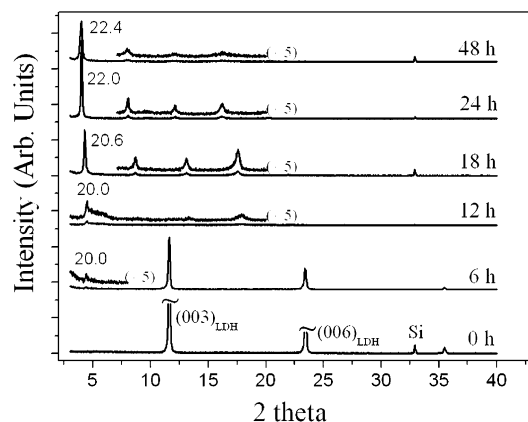


**Figure 1.** XRD spectra and basal spacings (Å) of PAA(L)-MgAl-LDH prepared in an ethanol/toluene mixture at 120 °C in various reaction periods.

to prepare the monolayer assembly of LDH nanocrystals on Si and Au-coated Si substrates, we need only 10 mg of LDH in 20 mL of 1-butanol using sonication treatment. The adhesion of LDH in this method shows a remarkable highly ordered 2D array on solid substrates, compared with simple solvent evaporation of colloidal dispersion, which gives random orientation.<sup>19</sup> The bonding between LDH and Si wafer is ascribed to the electrostatic attraction resulting from positively charged LDH particles and negatively charged Si substrate. We observed that the ultrasonic treatment exceedingly enhanced the coverage of LDH particles on the substrates without chemical linkers. We could also prepare a partially covered monolayer of zeolite microcrystals that was less dense than that of LDH when the ultrasonic treatment was performed with unmodified substrates, though Yoon et al.<sup>20</sup> demonstrated that the ultrasonic treatment worked well for the assembly of zeolite microcrystal monolayers with chemical linkers on glass substrates. Our report indicates that immobilization of the monolayered LDH nanocrystals on substrates is reliable only when using ultrasound without chemical linkers.

**PAA-LDH Nanocomposites.** Figure 1 presents the XRD data for the PAA(L)-LDH nanocrystals on Si in the solvothermal polymer incorporation as a function of reaction time. The peaks of pristine LDH remain after 6 h of reaction time, but disappear by 12 h. The PAA(L)-LDH nanocomposite materials consist of the LDH sheets stacking on top of each other, with interlayer gallery space being filled by polymeric guests. It is very surprising that the preferred crystallographic orientation of PAA(L)-LDH is confirmed by the strongly enhanced  $(00l)$  peaks up to  $l = 15$ . The basal spacings of PAA(L)-LDH range from 20.0 to 22.4 Å, suggesting that the interaction of acrylate anion within the gallery space is effective in the PAA(L)-LDH materials and that they increase up to 22.4 Å as the reaction times increase. The  $d$ -values around 22 Å are much larger than that value reported for other PAA(L)-LDH materials prepared in aqueous systems, 11.6–13.4 Å.<sup>9a</sup> The larger  $d$ -values observed are ascribed to packing of the molecular arrangements of PAA chains in

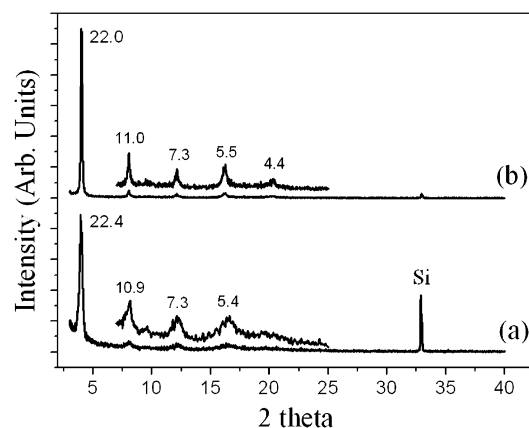


**Figure 2.** XRD spectra and basal spacings (Å) of (a) PAA(H)-MgAl-LDH for 48 h and (b) PAA(L)-MgAl-LDH for 24 h prepared in ethanol/toluene at 120 °C. The scale of the XRD spectra of (a) is multiplied by 4 to compare with that of (b).

the gallery space, partly due to the additional inclusion of water and the molecular conformation of PAA. The XRD spectra of the 24 h sample show the best crystalline quality among the prepared samples. The PAA incorporation in the LDH gallery space is likely very strong because the basal spacings do not change in the additional sonication treatments after the final washing step in ethanol solvents. We believe that the solvation of acids in alcohol media<sup>21</sup> and the preswelling with alcohol<sup>22</sup> play a critical role in the anion exchange because the carbonate form of LDH is difficult to exchange with other anions. A small amount of ethanol dissolves PAA to help the host–guest interaction in the reaction, even though ethanol dissolves LDH to decrease the crystallinity over a long contact time.

Through a solvothermal route, we successfully prepared PAA(L)-LDH hybrids on Si by adopting direct anion exchange of PAA with carbonate ions. As a novel synthetic method, the present reaction conditions do not require a nitrogen atmosphere to prevent the LDH samples from forming the carbonate LDH phase, which is indispensable in the previous coprecipitation synthesis in polymer solutions.<sup>10</sup> In addition, the coprecipitation and restacking methods thus far have some drawbacks, namely that the precipitate gives very poor crystallinity, limiting control of the reaction conditions such as polymer content without residual polymers in the composite materials.

Figure 2 demonstrates the comparison of reaction progress for PAA(L)-LDH and PAA(H)-LDH, indicating that PAA(L)-LDH has better crystallinity; this is probably ascribed to it having faster kinetics than PAA(H) because of the significantly different molecular weights of the two PAA molecules. An enlarged peak width in XRD spectra of PAA(H)-LDH is attributed to poorer crystallinity than that of PAA(L)-LDH, which is related to the fwhm (full width at half-maximum) values in  $2\theta$  for the main XRD peaks indicative of 0.24 and 0.30° for PAA(L)-LDH and PAA(H)-LDH, respectively. However, both PAA(L)-LDH and PAA(H)-LDH show same basal spacings at around 22 Å,

(19) (a) Ghosh, P. K.; Bard, J. *J. Am. Chem. Soc.* **1983**, *105*, 5691. (b) Itaya, K.; Chang, H. C.; Uchida, I. *Inorg. Chem.* **1987**, *26*, 624.  
(20) Lee, J. S.; Ha, K.; Lee, Y. -J.; Yoon, K. B. *Adv. Mater.* **2005**, *17*, 837.

(21) Fogg, A. M.; Green, V. M.; Harvey, H. G.; O' Hare, D. *Adv. Mater.* **1999**, *11*, 1466.

(22) Carlino, S. *Solid State Ionics* **1997**, *98*, 73.



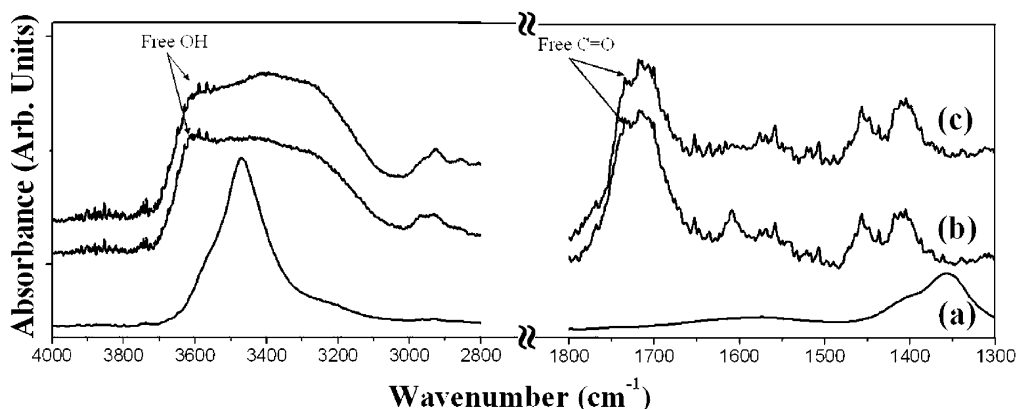


**Figure 3.** FT-IR spectra of pristine MgAl-LDH powder in (a) KBr, (b) PAA(L)-MgAl-LDH, and (c) PAA(H)-MgAl-LDH on Au-coated Si substrates. The intensities of (b) and (c) are multiplied by 5 to compare with that of (a).

indicating that the interlayer PAA molecules would be expected to involve similar conformations.

**FT-IR Spectra.** Figure 3 shows the FT-IR spectra for PAA(L)-LDH and PAA(H)-LDH on Au-coated silicon substrates, respectively, where similar characteristic bands were observed. The spectra for PAA(L)-LDH involve the peaks at 1436, 1560, and 1600  $\text{cm}^{-1}$ , corresponding to the symmetric and antisymmetric stretching modes of deprotonated carboxylic groups.<sup>15b</sup> Those for PAA(H)-LDH exhibit low intensities of the stretching modes of  $\text{COO}^-$  compared to that of the PAA(L)-LDH because of the significantly high molecular weight and some cross-linked polymer chains of PAA(H), which results in a poor crystallinity. The peaks at 2925 and 2850  $\text{cm}^{-1}$  are assigned to C–H stretching modes and one at 1460  $\text{cm}^{-1}$  to the scissoring mode. The bands at 1400–1420  $\text{cm}^{-1}$  are assigned to C–O stretching modes of the carboxylic group.<sup>15b,23</sup>

The strong vibration band observed at around 1730  $\text{cm}^{-1}$  is assigned to C=O stretching modes. The peak of 1710  $\text{cm}^{-1}$  exhibits the characteristic absorption peak corresponding to the inter- or intramolecular cyclic dimers with hydrogen bonding. The 1740  $\text{cm}^{-1}$  peak is assigned to free C=O without hydrogen bonding.<sup>23a</sup> The strong intensities of the observed bands are consistent with the presence of the incorporated PAA molecules involving intermolecular cyclic dimers and free carboxylic acids in the LDH gallery. Thus, the stretching modes of the hydroxyl group in pristine LDH come from the sharp peak at around 3500  $\text{cm}^{-1}$ , but the absorption corresponding to the OH stretching region in the PAA-LDH composites has a very unique broadband, extending up to 3700  $\text{cm}^{-1}$  in the high-frequency range. The presence of vibration frequencies ranging from 3500 to 3200  $\text{cm}^{-1}$  generally associated with OH stretching vibration results not only from a constrained environment surrounding acrylate anions, which are involved in a hydrogen-bonding network with the hydroxide layers and water molecules, but also from the hydrogen-bonding network between carboxylic acids. The peak at 3600  $\text{cm}^{-1}$  corresponds to the free OH stretching region,<sup>23</sup> supporting the existence of free C=O stretching modes. Since the characteristic absorption peaks

of interlayer PAA are shown in a higher frequency range than those observed in the starting poly(acrylic acid) (not shown), a high degree of freedom of the interlayer polyacrylic acids is expected. Besides, no carbonate anion is detected by IR spectroscopy, which proves that PAA entities are truly intercalated.

To investigate the existence of cyclic anhydride conformation<sup>24</sup> of PAA in the gallery, we applied the solvothermal treatment of PAA without MgAl-LDH on Au-coated silicon substrate in the same reaction conditions. The resulting polymer was condensed, and the IR spectra did not show any peaks from the ester carbonyl group, which confirms that the reaction condition presented here is incredibly effective for the incorporation of PAA with the original molecule conformation into the gallery space of LDH.

**Modeling of Interlayer PAA Arrangement in PAA-LDH.** Spectroscopic evidence suggests that PAA exists in different conformations depending on the solvent, pH, and ionic strength of the system.<sup>25</sup> PAA polymers could have a stretched or coiled conformation at the interface depending on the pH. The interlayer spacing for PAA was calculated by subtracting the LDH hydroxide layer thickness from the observed basal spacings, assuming a 4.8 Å thickness of LDH, the 22 Å observed value for PAA-LDH leads to a 17.2 Å of interlayer spacing for PAA molecules. This calculation suggested three different models, schematized in Figure 4.

First, we propose a multiple layer with a stretched conformation of PAA and polyacrylate chains (Figure 4a), similar to that observed in some LDH(Ni/Fe, Co)/polyacrylate complexes<sup>9a</sup> because of high charge density of LDH and high pH environments in the gallery space. In model (a), four layers of polymer are needed to extend to the 17.2 Å of interlayer expansion and the carboxylic groups of the polyacrylate chains are placed on the same side of the chain, facing one of the inorganic slabs, where two PAA chains connected with hydrogen bonding are located in between the two stretched polyacrylate chains in the center of the interslab space. The second model suggests preserving the PAA helical conformation in between the two stretched polyacrylate chains, as illustrated in Figure 4b. These

(23) (a) Daniliuc, L.; De Kesel, C.; David, C. *Eur. Polym. J.* **1992**, 28, 1365. (b) Fearheller, W. R., Jr.; Katon, J. E. *Spectrochim. Acta* **1967**, 22, 2225. (c) Shibaev, P. V.; Jensen, S. L.; Andersen, P.; Schaumburg, K.; Plaksin, V. *Macromol. Rapid Commun.* **2001**, 22, 493.

(24) (a) Yang, C. Q. *J. Polym. Sci., Part A: Polym. Chem.* **1993**, 31, 1187. (b) Yang, C. Q.; Wang, X. J. *J. Polym. Sci., Part A: Polym. Chem.* **1996**, 34, 1573.

(25) Arora, K. S.; Turro, N. J. *Polymer* **1986**, 27, 783.

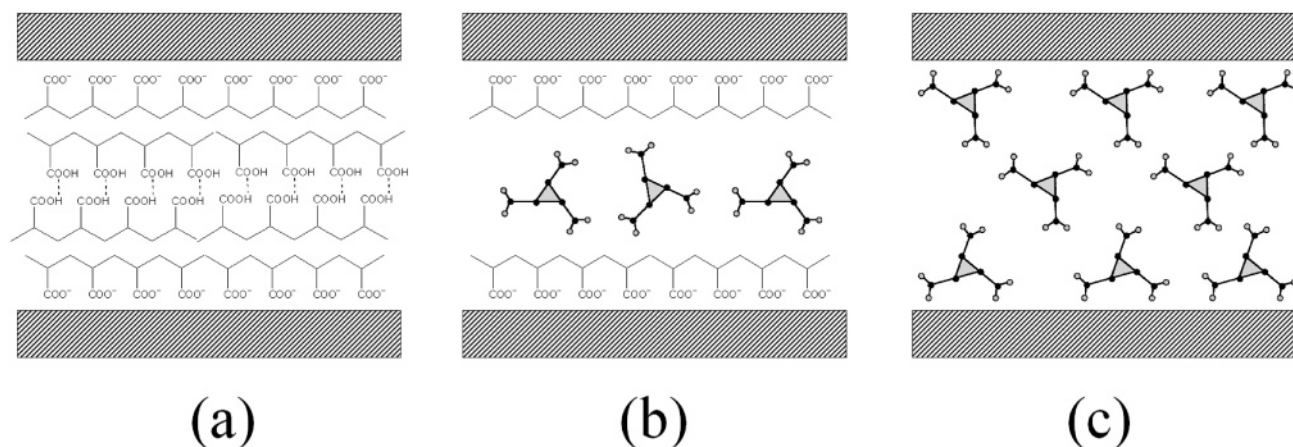
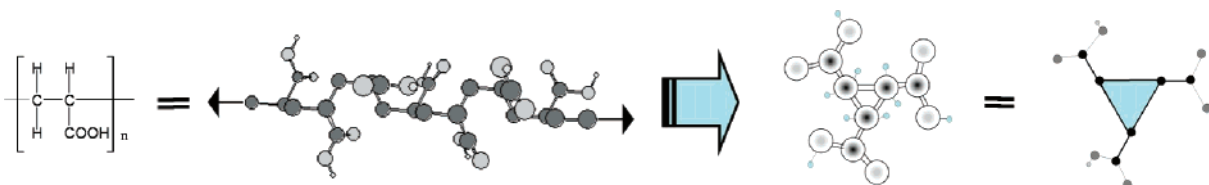


**Figure 4.** Suggested structural models for the prepared PAA-LDH composite materials: (a) well-ordered orientation of planar conformers, (b) planar and helical ones, and (c) three-layered helical ones (c).

**Scheme 1**



macromolecule conformations would indeed lead to a theoretical interlayer distance of around 17.2 Å. However, the bilayer conformations drawn in parts a and b of Figure 4b are not compatible with the results of the FT-IR spectroscopy because the characteristic absorption of COO<sup>-</sup> is remarkably weak in comparison with that of COOH. Other PAA-LDH nanocomposite materials prepared by in situ polymerization or coprecipitation in an aqueous solution<sup>9,10</sup> showed smaller basal spacing values and the strong characteristic absorption bands of COO<sup>-</sup>, suggesting the existence of a PAA bilayer in the LDH gallery. The data for the new PAA-LDH materials exclude the bilayer model, ascribed to the fact that the present samples have been prepared in nonaqueous solvents through the solvothermal route, resulting in the strong hydrogen-bonding networks among carboxylic groups.

The other possible model involves interlayer packing of PAA helical conformers, where the helices show three-turn (3<sub>1</sub>) helix conformation,<sup>26</sup> and two carboxylic groups of the PAA covering either side of LDH sheets confront with the hydroxide layers to compensate for the high charge density of LDH. The polymer helices are packed into the interlayer space with the axis of the polymer helix oriented parallel to the horizontal axes of Mg–Al hydroxide layers, as illustrated in Figure 4c. PAA helices alternately arranged in the middle of the interlayer space probably involve in the hydrogen-bonding network with the surrounding PAA helices. This conformation would also lead to a theoretical interlayer distance of around 17.2 Å. PAA molecules in aqueous solution as well as in dry and hydrated forms usually have random coil conformation due to strong association of the carboxylate moieties through hydrogen bonding.<sup>27</sup> Some

isotactic forms of many polyalkylacrylic acids are crystallized in the form of 3<sub>1</sub> helix conformation, as shown in Scheme 1. Considering the reaction temperature to be above the glass-transition temperature of PAA, e.g.,  $T_g < 106$  °C, and the reaction to take place in nonaqueous reaction media with less polarity and a high charge density of LDH, the helical conformation of PAA in the interlayer space is more likely than the bilayer structure of stretched polyacrylate. This interlayer packing would be regarded as a self-assembly process of polymer helices similar to the melting and recrystallization of polyethylene,<sup>28</sup> as the polymer remained in a reaction vessel was condensed; the dry form was thus hard and transparent.

Moreover, this hypothesis agrees with the result of the XRD spectra for a residual polymer, indicative of a distance between the polymer helices of around 5 Å, which is also compatible with the observed value for the starting PAA. This result well supports the proposed structure with three alternating layers of PAA helices. In particular, the ordered orientation of polymer–LDH involving the intercalated polymer is also supported by the strongly enhanced (001) reflections in XRD patterns for the PAA(L)-LDH as well as the PAA(H)-LDH with the same basal spacings.

We also note that the IR spectra for the new PAA-LDH nanocomposite film reveal the existence of free carbonyl (at 1740 cm<sup>-1</sup>) and free hydroxyl (at 3600 cm<sup>-1</sup>) groups, which means that the alternate packing of PAA helices in the gallery of LDH provides the high degree of freedom of interlayer

(26) (a) Bovey, F. A. *Polymer Conformation and Configuration*; Academic Press: New York, 1969; pp 73–97. (b) Natta, G. *Makromol. Chem.* **1960**, 35, 94.

(27) (a) Ravi, M.; Hopfinger, A. J. *J. Polym. Sci., Part B: Polym. Phys.* **1994**, 32, 1033. (b) Xu, X.; Carraher, C. E., Jr.; Jackson, M. D. In *Polymer Modification*; Proceedings of the ACS–PMSE Symposium on Polymer Modification, Orlando, FL, Aug 21–25, 1996; Swift, G., Carraher, C. E., Jr., Bowman, C. M., Eds.; Springer: New York, 1997; pp 165–170. (c) Kim, H. D.; Jin, S. H.; Lee, S. B.; Yang, J. S. *Polym. Bull.* **1997**, 31, 45.

(28) Yan, S.; Petermann, J. *Polymer* **2000**, 41, 6679.

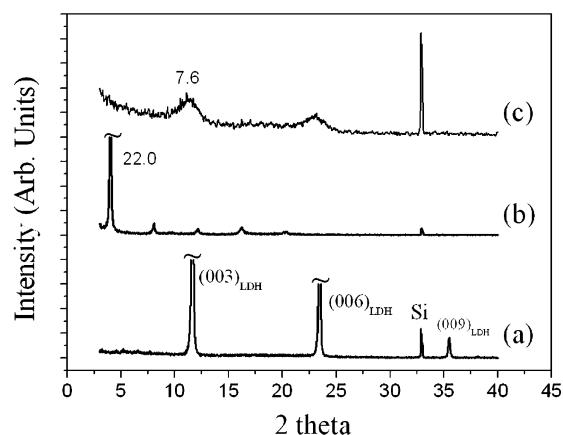


**Figure 5.** XRD spectra and basal spacings ( $\text{\AA}$ ) of (a) pristine MgAl-LDH on Si, (b) PAA(L)-MgAl-LDH/Si prepared by solvothermal treatment, and (c) after UV photodecomposition.

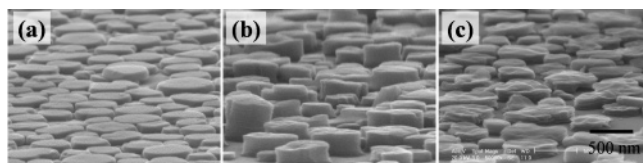


**Figure 6.** SEM images of (a) pristine MgAl-LDH on Si, (b) PAA(L)-MgAl-LDH/Si prepared, and (c) after UV photodecomposition.

polymer molecules. The IR spectra also exhibit a strong absorption of COOH in comparison with that of COO<sup>-</sup>, indicating that most of the PAA macromolecules in the interlayer space maintain their original conformation. Therefore, we suggest that the present system favors the interlayer packing of PAA helices in the form of alternate three layers, where the free form of carboxylic acids and intermolecular hydrogen-bonding network exist.

**UV-Light-Induced Patterning.** We were also interested in a photodecomposition of intercalated polymers under UV-light exposure. The UV-light irradiation using a high-pressure Hg lamp (600 W) of PAA(L)-LDH films leads to a change in the basal spacings in the XRD spectra, as shown in Figure 5c. The peaks for PAA(L)-LDH disappeared in 1 h under UV-light irradiation. The decrease in the  $d$ -value of PAA(L)-LDH to 7.6  $\text{\AA}$  was interpreted by complete photo-oxidation of the interlayer polymers<sup>9c</sup> and incorporation of carbonate ions, because the  $d$ -values around 7.6 and 3.8  $\text{\AA}$  are very similar to the values of a carbonate form of MgAl-LDH. The carbonate ions are most probably generated from incorporated carbon dioxides in air, because the present UV-decomposition condition does not prevent the carbon dioxides from forming a carbonate-LDH phase.

The particle morphology of LDH crystals on Si in each experimental step is demonstrated in Figure 6. The SEM image of PAA-LDH on Si showed remarkable anisotropic expansion of height with little change in horizontal width, presumably because it was expected that PAA molecules lift LDH slabs perpendicular to the Si surface. PAA-LDH on Si also exhibits sharp edges, indicating that the anion-exchange reaction using a small amount of alcohol may have little influence on the crystallinity of LDH layers. The reaction conditions presented here provide polymer-free surfaces, usually difficult to obtain in powdery samples, signifying that the reaction media may minimize surface adsorption of

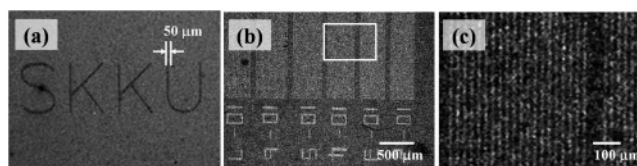


**Figure 7.** Optical microscopic images of PAA-LDH/Si after UV radiation through (a) stainless steel shadow mask prepared by laser cutting and (b) Cr metal-photo mask on quartz glass to produce micropatterns; (c) enlarged image of the selected area in (b).

polymer; thus, residual polymers are readily removed from the LDH surfaces. The PAA-LDH samples after UV treatments collapse their heights by decomposition of PAA in the gallery space of LDH with corrugated surface morphology. The nonconformal surfaces of PAA-LDH and UV-treated PAA-LDH samples are related by the destruction of crystallinity, which is corroborated by enlarged peak widths in XRD data. The fwhm values in  $2\theta$  for the main XRD peaks were 0.12, 0.24, and 0.54° for pristine LDH, PAA(L)-LDH, and UV-treated PAA-LDH, respectively.

UV-light irradiation also leads to a color change from white gray in the PAA-LDH film to dark gray in the UV-treated PAA-LDH film, which was applied to a light-induced patterning. Note that the work presented here represents two-dimensional microstructures of polymer-inorganic hybrid films prepared by the light-induced patterning process. Through UV-light exposure, we successfully prepared the micropatterned structures of PAA-LDH composite films by UV decomposition of the interlayer polymer, as shown in Figure 7. The UV-light exposure of the as-made PAA(L)-LDH was carried out with a metal mask and a quartz photo mask. The patterned PAA-LDH sample as shown in Figure 7a was prepared using a metal mask with a hollow space 50  $\mu\text{m}$  in width, and the one in Figure 7b was prepared using a quartz photo mask with Cr patterns 10  $\mu\text{m}$  in width. Figure 7c shows an enlarged image of the selected area in Figure 7b, which indicates the well-defined micropatterns of PAA-LDH film with a 10  $\mu\text{m}$  line width. In these images, the dark regions correspond to the UV-decomposed PAA-LDH area, and the bright regions correspond to the intact PAA-LDH area. This patterned PAA-LDH film resulted from the selective photodecomposition of interlayer PAA and the collapse of LDH slabs perpendicular to the Si surface during the UV exposure.

## Conclusions

This approach to the intercalation chemistry of polymer guest demonstrates a novel synthetic method of PAA/LDH hybrid composite films by the direct incorporation of PAA macromolecules. The ethanol/toluene mixture system prevents dissolution of LDH and preserves the layered structure of immobilized LDH on Si during the polymeric anion-exchange reaction. The intercalation of PAA and its interlayer conformation are clearly inferred from the XRD and IR data. The strongly enhanced ( $00l$ ) harmonics in the XRD spectra for the PAA-LDH films indicate the highly ordered orientation of polymer-inorganic materials involving well-ordered interlayer arrangements. The IR spectra suggest that the three-layered helical conformation of the interleaved PAA is the

most probable model. In addition, the light-induced micro-patterning of PAA-LDH films could be readily performed by UV exposure using a photo mask as well as a metal shadow mask. This result involves the photodecomposition of interlayer polymer and, finally, the collapsing of LDH slabs perpendicularly to the substrate. We believe that the well-ordered polymer-LDH hybrid films and their micro-structures potentially provide a wide range of opportunities for optical devices, clay-modified electrodes, and chemical

sensor applications, because they are expected to be useful and attractive candidates in comparison to the powdery samples investigated in this area prior to now.

**Acknowledgment.** This work was supported by the KISTEP (Program M1-0214-00-0228), the BK-21 program, and the Korea Research Foundation Grant funded by the Korean Government (MOEHRD) (KRF-2005-005-J11902).

CM060278B